

# MAGELLAN SPECTROSCOPY OF THE GALAXY CLUSTER RX J1347.5–1145: REDSHIFT ESTIMATES FOR THE GRAVITATIONALLY LENSED ARCS

SWARA RAVINDRANATH<sup>1,2</sup> AND LUIS C. HO<sup>1</sup>

*To appear in The Astrophysical Journal, September 2002*

## ABSTRACT

We present imaging and spectroscopic observations of the gravitationally lensed arcs in the field of RX J1347.5–1145, the most X-ray luminous galaxy cluster known. Based on the detection of the [O II]  $\lambda 3727$  emission line, we confirm that the redshift of one of the arcs is  $z = 0.806$ . Its color and [O II] line strength are consistent with those of distant, actively star forming galaxies. In a second arc, we tentatively identify a pair of absorption lines superposed on a red continuum; the lines are consistent with Ca II  $\lambda 3933$  (K) and Ca II  $\lambda 3968$  (H) at  $z = 0.785$ . We detected a faint blue continuum in two additional arcs, but no spectral line features could be measured. We establish lower limits to their redshifts based on the absence of [O II] emission, which we argue should be present and detectable in these objects. Redshifts are also given for a number of galaxies in the field of the cluster.

*Subject headings:* galaxies: clusters: individual (RX J1347.5–1145) — galaxies: distances and redshifts — gravitational lensing

## 1. INTRODUCTION

Gravitational lensing by galaxy clusters serves as a powerful probe of cosmological structure. The lensing phenomenon provides information on both the mass distribution of the lensing cluster and the nature of the background population of faint field galaxies (e.g., Smail et al. 1993; Fort & Mellier 1994). Measurements of cluster mass also place useful constraints on the nature of dark matter and the cosmological parameter  $\Omega$  (e.g., Mellier, Fort, & Kneib 1993; Fort & Mellier 1994; Crone, Evrard, & Richstone 1994, 1996; White & Fabian 1995). The arcs that are often seen in deep images of galaxy clusters are the sheared and magnified images of faint, background galaxies (Paczynski 1987). The amplification provided by gravitational lensing enables spectroscopic studies of these faint galaxies, which would otherwise be extremely difficult, if not impossible. The spectra of the arcs yield information on the redshifts and stellar populations of the lensed galaxies (e.g., Smail et al. 1993; Bézecourt & Soucaïl 1997; Ebbels et al. 1998; Hall et al. 2000; Campusano et al. 2001). The redshifts of the arcs constrain models of the cluster potential and provide robust estimates of the total cluster mass.

RX J1347.5–1145, at a redshift of 0.451, is the most luminous X-ray cluster known, with an X-ray luminosity in excess of  $10^{45}$  erg s<sup>−1</sup> (Schindler et al. 1995, 1997; Ettori, Allen, & Fabian 2001). The mass estimates based on its X-ray properties (Schindler et al. 1995), the Sunyaev-Zel’dovich effect (Pointecouteau et al. 1999), weak-lensing models (Fischer & Tyson 1997), and strong-lensing models (Sahu et al. 1998; Cohen & Kneib 2002) have yielded discrepant results for the total mass of this cluster. Cohen & Kneib (2002) speculate that we may be witnessing the merging of two clusters along a direction perpendicular to our line of sight.

Strong constraints can be placed on the cluster mass based on the redshifts of lensed background galaxies. Schindler et al. (1995) discovered an arc system in RX J1347.5–1145; it comprises of two bright arcs located  $\sim 35''$  from the central dominant galaxies, at diametrically opposite points along the North-

South direction. This was confirmed by the observations of Fischer & Tyson (1997). For the bright northern arc (Arc 1), Sahu et al. (1998) reported the detection of an emission line plausibly identified with [O II]  $\lambda 3727$  at a redshift of 0.81. The bright southern arc (Arc 4) showed a faint blue continuum but no spectral line features. The high-resolution *Hubble Space Telescope* images of Sahu et al. (1998) also revealed three additional arcs in this cluster (Arcs 2, 3, and 5). Figure 1 shows an *R*-band image of the central region of the cluster with identification for the five arcs.

This paper presents new photometry and spectroscopy of the arc system in RX J1347.5–1145. We confirm the emission-line redshift previously reported for Arc 1, report the tentative detection of an absorption-line redshift for Arc 2, and give limits on the redshifts of Arcs 3 and 4. These measurements are in good agreement with the predictions from the lensing models of this cluster. We also give redshifts for a number of galaxies in the field of the cluster.

## 2. OBSERVATIONS AND DATA REDUCTIONS

In preparation for the spectroscopic observations, on 2001 February 20 UT we acquired relatively deep *V* ( $2 \times 1200$  s) and *I* ( $2 \times 900$  s) images of RX J1347.5–1145 using the 2.5-m du Pont telescope at Las Campanas Observatory. The CCD was a thinned Tektronics  $2048 \times 2048$  chip with a pixel scale of  $0''.26$ , a gain of  $3.0 e^-$  per ADU, and a read noise of  $7 e^-$ . The data were taken under photometric, sub-arcsecond ( $\sim 0''.8$ ) conditions. The images were used for photometry of the arcs and to obtain accurate relative astrometry for the preparation of the slit mask for the spectroscopic observations. Photometric and astrometric calibrations were achieved by observing the open cluster M 67 (Montgomery, Marschall, & Janes 1993).

We obtained spectra of the brightest four arcs (Arcs 1–4 in the notation of Sahu et al. 1998) on 2001 May 15–16 UT, using the multislit LDSS-2 spectrograph (Allington-Smith et al. 1994) mounted on the 6.5-m Magellan I (Baade) telescope at Las Campanas. We did not include Arc 5 because it partly over-

<sup>1</sup>The Observatories of the Carnegie Institution of Washington, 813 Santa Barbara St., Pasadena, CA 91101-1292.

<sup>2</sup>Department of Astronomy, University of California, Berkeley, CA 94720-3411.

laps with Arc 1 along the dispersion direction. The

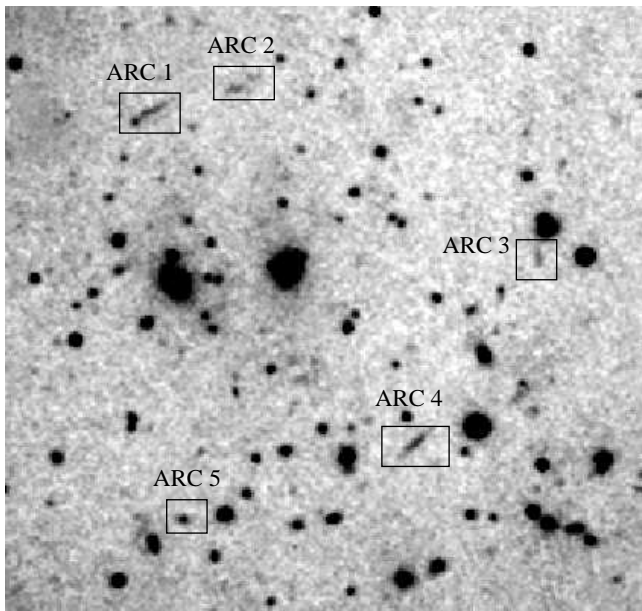


FIG. 1.— The *R*-band acquisition image of RX J1347.5–1145 obtained using LDSS-2 on the Baade telescope. The gravitationally lensed arcs are identified using the notation of Sahu et al. (1998). The field shown here covers a  $1.8' \times 1.8'$  region centered around the dominant cluster galaxies. North is to the top and East is to the left.

300 line  $\text{mm}^{-1}$  grism blazed at  $6000 \text{ \AA}$  covered the spectral range  $\sim 4000$  to  $8000 \text{ \AA}$  with a dispersion of  $5.3 \text{ \AA pixel}^{-1}$ . The two-dimensional spectra were recorded on a SiTe  $2048 \times 2048$  CCD, which has a spatial resolution of  $0''.38 \text{ pixel}^{-1}$ . In order to maximize the light input from the faint, low surface brightness arcs ( $\mu_V \approx 25 - 26 \text{ mag arcsec}^{-2}$ ), we chose the width of the slits to be  $2''$ . This gave a full width at half maximum (FWHM) spectral resolution of  $25 \text{ \AA}$ . For simplicity, all the slits were oriented along the East-West direction, at the expense that for most of the arcs only a portion of each object intersected with the slit. The slits were required to have a minimum length of  $10''$  in order to have enough area for sky subtraction. In addition to the arcs, the mask also contained slits for a number of galaxies that were likely to be associated with the cluster. The total integration time was  $21,400 \text{ s}$  ( $\sim 6 \text{ hr}$ ), split into seven roughly equal exposures. The sky conditions were clear, the atmospheric seeing varied between  $0''.6$  and  $0''.9$ , and the airmass ranged from  $1.0$  to  $1.65$ .

The basic data reductions were carried out using the IRAF<sup>4</sup> package. The du Pont images were bias-subtracted, flat-fielded with twilight skyflats, aligned, and then median combined after cosmic-ray rejection. Photometry of the arcs and galaxies was performed using the SExtractor software (Bertin & Arnouts 1996), which uses elliptical apertures to compute magnitudes within an isophotal radius that is twice the first-moment radius (Kron 1980). The maximum radius used to compute the first-moment radius corresponds to an isophotal value that is  $1.5 \sigma$  of the background. The formal errors on the magnitudes derived from SExtractor are  $\sim 0.3 \text{ mag}$ . The magnitudes were corrected for atmospheric extinction and transformed to the standard Johnson system using calibrations derived from photometry of the standard stars in M 67.

The spectroscopic frames were corrected for the overscan, flat-fielded with domeflats, aligned, and then median combined after cosmic-ray rejection. Accurate sky subtraction proved to be challenging especially for the lensed arcs. This is in part due to the extremely low surface brightness of the arcs and to the fact that the spectra are slightly tilted. After some experimentation, we found that two-dimensional background subtraction gave the most robust results. The background was estimated by fitting a third-order Chebyshev polynomial along the columns using all the rows excluding those that contain the object spectrum. We extracted one-dimensional spectra by summing the central 10 rows ( $\sim 4''$ ); this extraction width was determined empirically to give the best signal-to-noise ratio (S/N). We established the wavelength scale by fitting a third-order polynomial to unblended emission lines of He and Ne in the comparison lamp spectra. Finally, the relative fluxes of the spectra were calibrated using longslit observations of the standard stars LTT 7987 and LTT 9491 (Stone & Baldwin 1983). Note that we did not attempt to perform absolute spectrophotometry because our primary goal was to obtain redshifts for the arcs and galaxies.

### 3. PROPERTIES OF THE ARCS

Table 1 summarizes the integrated magnitudes and colors obtained from the broad-band images. Figure 2 shows the final spectra for the lensed arcs in RX J1347.5–1145. For each arc, we present both the two-dimensional background-subtracted spectrum (in greyscale) and the extracted, calibrated one-dimensional spectrum.

The spectrum of Arc 1 shows an unresolved emission line centered at  $\sim 6728 \text{ \AA}$ . The emission-line knot is clearly visible in the two-dimensional sky-subtracted image, and it is unmistakable in each of the sub-exposures. This line was already reported by Sahu et al. (1998), who argued that it is likely to be redshifted [O II]  $\lambda 3727$ . Adopting this interpretation gives a redshift of  $0.806$ . The line has an equivalent width (EW) of  $85 \pm 10 \text{ \AA}$ , where the error bars reflect uncertainties in the placement of the continuum level and in whether the line flux is measured by direct integration or profile fitting. We note that although our absolute fluxes are not reliable because of slit losses, the EW measurements are likely to be more robust, so long as there are not large spatial variations of the line-emitting regions within the galaxy. From the photometry, we measure a moderately red color of  $V - I \approx 1.6 \text{ mag}$ , similar to the color  $B_J - R = 1.1 \text{ mag}$  given by Fischer & Tyson (1997).

Arc 2, for which there have been no previous spectroscopic observations, exhibits a pair of absorption lines at  $7017$  and  $7084 \text{ \AA}$  superposed on a relatively red continuum. The color derived from the images is also rather red, with  $V - I \approx 2.7 \text{ mag}$ . The lines fall on a fairly clean part of the spectrum and do not appear to be adversely affected by sky subtraction.

We clearly detected the continuum in Arcs 3 and 4, but the spectra do not reveal any distinct emission or absorption features that can provide a direct redshift measurement. The feature near  $5200 \text{ \AA}$  in the spectrum of Arc 4 appears not to be real. It is not seen in the background-subtracted two-dimensional image and may have resulted from the addition of significant residuals within the extraction aperture. The spectrum of Arc 3 is substantially noisier than that of Arc 4, for two reasons. First, Arc 3 is  $\sim 1.5 \text{ mag}$  fainter. And second, the slit was oriented

<sup>4</sup>IRAF is distributed by the National Optical Astronomy Observatories, which are operated by the Association of Universities for Research in Astronomy, Inc., under cooperative agreement with the National Science Foundation.

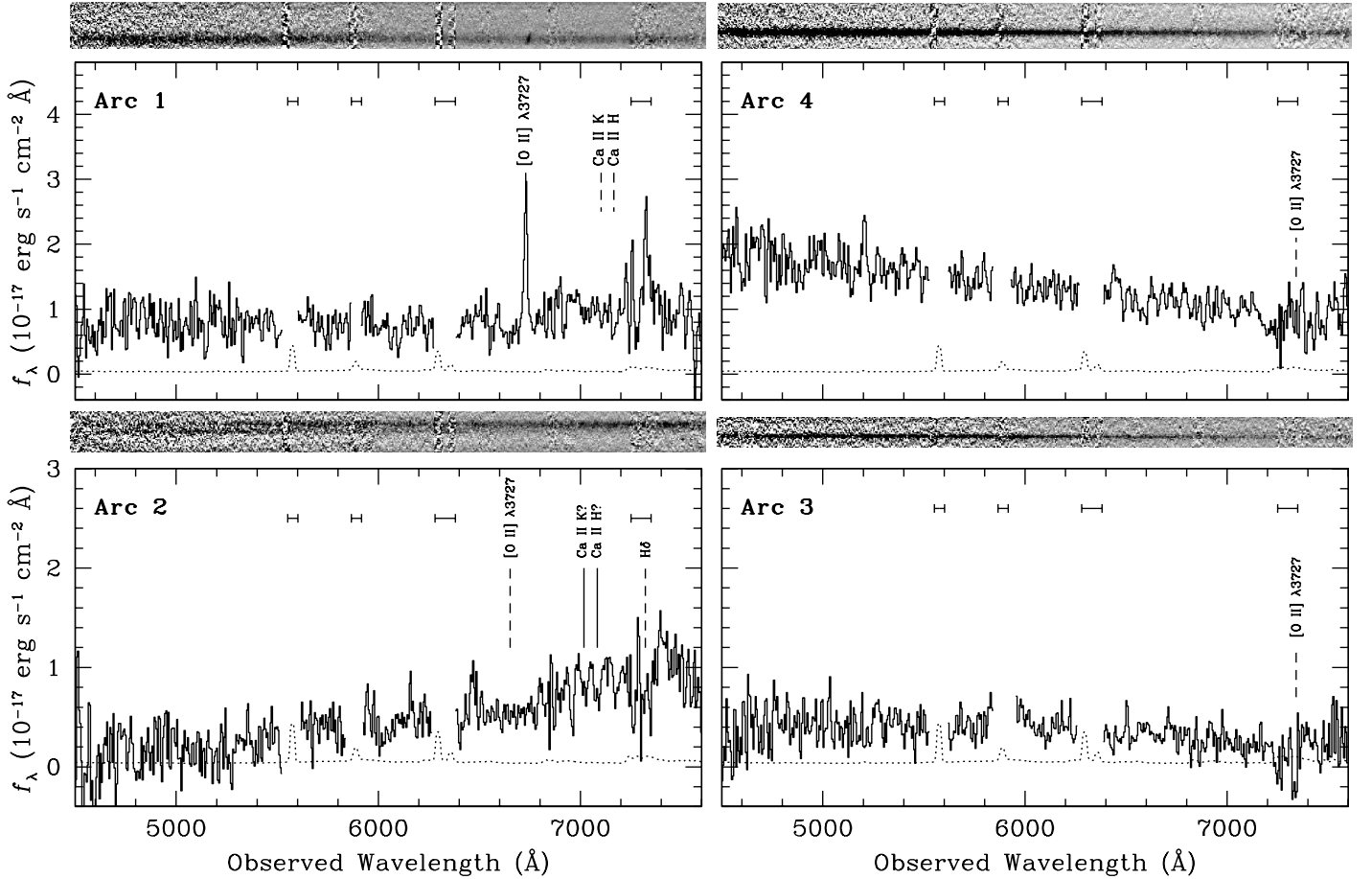


FIG. 2.— Spectra of the gravitational arcs in RX J1347.5–1145. For each arc, its two-dimensional sky-subtracted spectrum (in greyscale) is shown along with the one-dimensional extracted spectrum; both cover the same wavelength range (4500–7600Å). The dotted line in each panel shows the sky spectrum, scaled by a factor of 0.01. The gaps in the object spectrum corresponds the positions of strong sky lines (indicated by bars) where imperfect sky subtraction leaves large residuals. The spectral features used to infer the redshifts are marked with solid lines, while the dashed lines mark the positions of other features expected for the inferred redshifts. In the spectra of Arc 3 and 4, we marked the position of [O II]  $\lambda 3727$  expected for  $z = 0.97$ , as predicted by Allen et al. (2002).

in an especially unfavorable position angle with respect to the object; the length of the arc runs North-South (see Fig. 1), exactly orthogonal to the slit. Arcs 3 and 4 are significantly bluer than Arcs 1 and 2. We measure  $V - I \approx 0.41$  and  $0.58$  mag for Arcs 3 and 4, respectively; for comparison, Fischer & Tyson (1997) give  $B_J - R = 0.4$  mag for Arc 4.

#### 4. REDSHIFTS FOR GALAXIES IN THE FIELD OF RX J1347.5–1145

We obtained spectra for 22 galaxies in the field of the cluster; Table 2 gives redshifts and basic photometric data for 21 of these. The galaxy redshifts were determined using the cross-correlation technique of Tonry & Davis (1979) as implemented in the *xcsao* task in IRAF. Cross-correlation templates were taken from the spectrophotometric atlas of galaxies of Kenicutt (1992a). These templates cover the wavelength range 3650–7100 Å at a resolution of 5–8 Å. We correlated each galaxy spectrum with a set of seven template spectra chosen to represent a range of spectral types. The templates include NGC 3379 (E1), NGC 4472 (E2), NGC 4889 (E4), NGC 3921 (S0/a), NGC 3627 (Sb), NGC 6764 (Sbc), and NGC 6240 (I0). NGC 3921 has a post-starburst spectrum showing a mixed population

with strong Balmer absorption lines typical of A stars along with K-giant features. Both absorption-line and emission-line templates were used for redshift determination, depending on the spectrum of the observed galaxy.

The two main contributions to the errors in the measured redshifts arise from template mismatch and errors in the wavelength calibration. The errors due to template mismatch can be estimated from the dispersion in the final redshifts resulting from different input templates. For redshifts based on absorption-line templates, these errors are typically  $\sim 350$  km  $s^{-1}$ . The errors are significantly smaller when the redshifts are determined using emission-line templates, with  $\sim 100$  km  $s^{-1}$  being a typical value. The rms error in the wavelength calibration of our observed galaxy spectra was found to be  $\sim 5$  Å. Adding the two contributions in quadrature, we estimate a total error of  $\sim 0.0014$  for the derived redshifts. In addition, there can be errors in the velocity zeropoints due to wavelength calibration errors of the template galaxy spectra. However, these are of the order of few tens of km  $s^{-1}$  (Yee, Ellingson, & Carlberg 1996), and we have not included them in our error estimation.

TABLE 1  
MEASURED PROPERTIES OF THE ARCS

Arc	$V$ (mag)	$V - I$ (mag)	$\mu_V$ (mag arcsec $^{-2}$ )	Redshift
(1)	(2)	(3)	(4)	(5)
1	22.3	1.6	25.9	0.806
2	23.6	2.7	25.4	0.785
3	23.1	0.41	24.9	>1.04
4	21.5	0.58	25.3	>0.93
5	22.7	0.54	25.3	...

NOTE.— Col. (1) Identification number of the arc (see Fig. 1). Col. (2) Integrated  $V$ -band magnitude. Col. (3) Integrated  $V - I$  color. Col. (4)  $V$ -band surface brightness. Col. (5) Observed redshift; limits on the redshift are based on the apparent absence of [O II]  $\lambda 3727$  at  $\sim 7600$  Å.

Our redshift estimates show excellent agreement with the results reported by Cohen & Kneib (2002) in the case of four galaxies common to both studies. We assign cluster membership based on the velocity distribution presented by Cohen & Kneib (2002) for 47 spectroscopically confirmed cluster members. Five galaxies in our study have redshifts close to the redshifts for the two central cD galaxies given by Cohen & Kneib (2002), and thus are likely to be cluster members. Among these, the galaxy with  $z = 0.431$  is at the tail end of the velocity distribution, but we include it as a cluster member because its red  $V - I$  color is similar to that of the other cluster galaxies. Another probable cluster member is a galaxy at redshift  $z = 0.426$  that lies close to the range spanned by the velocity distribution. This galaxy shows an absorption-line spectrum, but its  $V - I$  color is relatively blue compared to the other cluster members. Only one of the galaxies among the likely cluster members, G47195–4344, shows an emission-line spectrum; it is located at the outskirts of the cluster,  $\sim 3'$  from the central cD galaxies. A similar cluster member candidate was reported by Cohen & Kneib (2002); C47229\_4519 has a relatively blue color and is the only cluster galaxy in their sample other than the central cD galaxy (which hosts an active nucleus) to show the [O II]  $\lambda 3727$  emission line.

## 5. DISCUSSION AND SUMMARY

Our primary aim is to determine or place limits on the redshifts of the arcs in RX J1347.5–1145. The redshift for Arc 1 is relatively secure. Consistent with the study of Sahu et al. (1998), we detected a strong emission line at  $\sim 6728$  Å whose most likely identification is [O II]  $\lambda 3727$  at  $z = 0.806$ . As discussed by Sahu et al. (1998), Ly $\alpha$   $\lambda 1216$  or C IV  $\lambda 1550$  can be ruled out based on the photometric colors: the Lyman limit would render the  $B_J - R$  color much redder than that reported by Fischer & Tyson (1997). More directly, our spectrum, which extends to  $\sim 4500$  Å, shows no sign of any continuum decrement. Strong optical lines such as H $\beta$ , [O III]  $\lambda \lambda 4959, 5007$ , or H $\alpha$  can be ruled out trivially by the redshift (0.451) of the lensing cluster.

The detection of the [O II] line allows us to deduce a few basic properties concerning Arc 1. The measured [O II] EW of  $\sim 75$ – $95$  Å compares well with values previously found in gravitationally lensed arcs seen toward other galaxy clusters (Ebbels et al. 1998). It is somewhat larger than in typical nearby late-type galaxies (EW  $\approx 50$  Å; Kennicutt 1992b), but lies in the upper end of the EW distribution seen in distant, faint galaxy samples (e.g., Colless et al. 1990; Hammer et al. 1997). The observed  $V - I$  color is also consistent with that ex-

pected for the faint blue galaxy population at  $z \approx 0.8$  (Forbes et al. 1996). Although slit losses prevent us from measuring accurate total fluxes, we can use the observed [O II] emission-line flux to set a lower limit to the formation rate of massive (ionizing) stars. Kennicutt (1998) gives the following empirical relation between [O II] luminosity ( $L_{\text{[O II]}}$ ) and star formation rate (SFR):

$$\text{SFR}(M_{\odot} \text{ yr}^{-1}) = (1.4 \pm 0.4) \times 10^{-41} L_{\text{[O II]}} (\text{erg s}^{-1}). \quad (1)$$

This derivation assumes a Salpeter (1955) stellar initial mass function and solar metallicity. For an observed  $F_{\text{[O II]}} > 5.5 \times 10^{-16} \text{ erg s}^{-1} \text{ cm}^{-2}$  and cosmological parameters  $H_0 = 75 \text{ km s}^{-1} \text{ Mpc}^{-1}$ ,  $\Omega_m = 0.3$ , and  $\Omega_{\Lambda} = 0.7$ , we obtain  $\text{SFR} > 24 M_{\odot} \text{ yr}^{-1}$ . The above calculation accounts for a Galactic extinction of  $A_B = 0.268 \text{ mag}$  (Schlegel, Finkbeiner, & Davis 1998) corrected using the extinction law of Cardelli, Clayton, & Mathis (1989). To obtain the *intrinsic* SFR, we need to know the flux magnification factor due to the lensing. According to the lensing model of Allen, Schmidt, & Fabian (2002), the magnification factor of Arc 1 is 7.7 (R. W. Schmidt, private communication). Thus, the true lower limit to the SFR for Arc 1 is  $\sim 3 M_{\odot} \text{ yr}^{-1}$ . This is comparable to the level of star formation activity in nearby gas-rich spiral galaxies (e.g., Kennicutt 1983) but is significantly lower than those obtained for the arcs in Abell 2218 (Ebbels et al. 1996) and Abell 2390 (Bézecourt & Soucaill 1997; Lémonon et al. 1998). It is unclear whether slit losses alone can make up for the difference.

For Arc 2, we tentatively identify the pair of absorption lines at 7017 and 7084 Å with Ca II  $\lambda 3933$  (K) and Ca II  $\lambda 3968$  (H) at a redshift of 0.785. This interpretation is plausible considering (1) the redness of the continuum, which is suggestive of an old stellar population, and (2) the absence of any strong emission lines blueward of the absorption lines. An old stellar population should show a more prominent 4000 Å break than observed, but the shape of the spectrum redward of  $\sim 7200$  Å is too uncertain (due to telluric molecular absorption bands and residuals from subtraction of sky lines) to be definitive on this point. For an elliptical galaxy at  $z \approx 0.8$ , the observed  $V - I$  color of 2.7 mag corresponds to a present-day restframe  $V - I \approx 1.2 \text{ mag}$  (Poggianti 1997), consistent with the colors of local elliptical galaxies (e.g., Fukugita, Shimasaku, & Ichikawa 1995). Allen et al. (2002) recently used *Chandra* data to refine the mass model for RX J1347.5–1145. Adjusting their model to reproduce the redshift measurement of Arc 1 by Sahu et al. (1998), Allen et al. (2002) predict the redshifts of the other arcs. For Arc 2, they give  $z = 0.75 \pm 0.05$ , in excellent agreement with our value.

Allen et al. (2002) predict  $z = 0.97 \pm 0.05$  for Arcs 3 and

TABLE 2: PROPERTIES OF GALAXIES IN THE FIELD OF RX J1347.5-1145

ID	V	V - I	z	Spectral Type	Remarks
(1)	(mag)	(mag)	(4)	(5)	(6)
G47177-4556	18.8	1.6	0.087	A	a
G47195-4344	21.2	1.1	0.445	E	CG
G47202-4501	21.5	1.2	0.259	E	
G47205-4329	21.1	2.2	0.350	A	
G47218-4233	22.3	1.4	0.336	A	b
G47232-4435	22.0	1.7	0.426	A	CG?
G47238-4606	22.8	1.1	0.397	E	
G47251-4357	21.6	1.4	0.266	A	
G47260-4441	21.0	1.9	0.691	E+A	
G47338-4140	21.9	2.1	0.455	A	CG
G47343-4519	20.7	1.4	0.201	A	b
G47356-4602	19.0	1.3	0.086	E	
G47358-4129	21.9	2.4	0.431	A	CG
G47368-4329	21.7	1.5	0.408	E	
G47382-4444	21.4	2.6	0.449	A	CG
G47397-4401	21.0	2.2	0.349	A	
G47402-4241	20.2	1.0	0.192	A	b
G47411-4340	20.6	2.2	0.348	A	
G47417-4449	21.3	2.5	0.457	A	CG
G47424-4528	22.1	1.7	0.662	E	c
G47426-4256	22.2	2.4	0.591	E+A	

NOTE.— Col. (1) Galaxy identification names based on the coordinates; Gmmss- $\alpha\alpha\beta\beta$  represents the position R.A.(J2000) = 13 mm ss.s and Dec.(J2000) = -11  $\alpha\alpha\beta\beta$ . Col. (2) Integrated V-band magnitude. Col. (3) Integrated V - I color. Col. (4) Measured redshift. Col. (5) Spectral type: E = emission-line spectrum; A = absorption-line spectrum; E+A = post-starburst spectrum. Col. (6) Remarks: CG = cluster member; a = H $\alpha$ + [N II]  $\lambda\lambda$ 6548, 6583 and [S II]  $\lambda\lambda$ 6716, 6731 are present; b = [O II]  $\lambda$ 3727 is present; c = uncertain redshift based on a single emission line, assumed to be [O II]  $\lambda$ 3727.

4. Since both of these objects have featureless continua very similar in shape to that of Arc 1 — indeed, they are *bluer*, suggesting an even younger stellar population — it is reasonable to expect that nebular emission should be present at a comparable, if not even greater, strength. However, no significant emission feature is discernible at  $\sim 7340$  Å, the expected location of [O II] at  $z = 0.97$ . Unfortunately, the quality of the spectrum in the region  $\sim 7300$ – $7400$  Å is degraded by imperfect removal of the OH sky lines (see, e.g., Osterbrock & Martel 1992). Nevertheless, a narrow emission feature with a strength comparable to that of the [O II] line in Arc 1, and perhaps even a factor 2–3 weaker, would almost certainly have been detected in Arc 4, since the two objects have virtually identical continuum levels. These arguments suggest that the redshift of Arc 4 is greater than 1.04, where we have taken the upper limit of our bandpass to be 7600 Å. This redshift limit does not appear to be in serious conflict with the predicted value.

The faintness of Arc 3 makes its spectrum highly uncertain at

the red end, and we limit our discussion to wavelengths  $\lesssim 7200$  Å, where the continuum is clearly detected and not severely affected by systematic effects. The absence of any emission features with equivalent widths greater than  $\sim 10$  Å suggests that the redshift is likely to be larger than 0.93. This is consistent with the value predicted by Allen et al. (2002).

This work is funded by NASA LTSA grant NAG 5-3556 and by NASA grants HST-AR-07527.03-A and HST-AR-08361.02-A from the Space Telescope Science Institute (operated by AURA, Inc., under NASA contract NAS5-26555). We are grateful to Paul Martini for obtaining the broad-band images of the cluster. We thank Andrew McWilliam, Patrick McCarthy, and Daniel Kelson for helpful discussions on the spectroscopic reductions. Robert Schmidt kindly communicated the magnification factors for the arcs. An anonymous referee gave helpful suggestions for improving the paper.

## REFERENCES

- Allen, S. W., Schmidt, R. W., & Fabian, A. C. 2002, MNRAS, in press (astro-ph/0111368)  
Allington-Smith, J., et al. 1994, PASP, 106, 983  
Bertin, E., & Arnouts, S. 1996, A&AS, 117, 393  
Bézecourt, J., & Soucail, G. 1997, A&A, 317, 661  
Campusano, L. E., Pelló, R., Kneib, J.-P., Le Borgne, J.-F., Fort, B., Ellis, R., Mellier, Y., & Smail, I. 2001, A&A, 378, 394  
Cardelli, J. A., Clayton, G. C., & Mathis, J. S. 1989, ApJ, 345, 245  
Cohen, J. G., & Kneib, J.-P. 2002, ApJ, in press (astro-ph/0111294)  
Colless, M., Ellis, R. S., Taylor, K., & Hook, R. N. 1990, MNRAS, 244, 408  
Crone, M. M., Evrard, A. E., & Richstone, D. O. 1994, ApJ, 434, 402  
—. 1996, ApJ, 467, 489  
Ebbels, T. M. D., Ellis, R. S., Kneib, J.-P., Le Borgne, J.-F., Pelló, R., Smail, I., & Sanahuja, B. 1998, MNRAS, 295, 75  
Ebbels, T. M. D., Le Borgne, J.-F., Pelló, R., Ellis, R. S., Kneib, J.-P., Smail, I., & Sanahuja, B. 1996, MNRAS, 281, L75  
Ettori, S., Allen, S. W., & Fabian, A. C. 2001, MNRAS, 322, 187  
Fischer, P., & Tyson, J. A. 1997, AJ, 114, 14  
Forbes, D. A., Phillips, A. C., Koo, D. C., & Illingworth, G. D. 1996, ApJ, 462, 89  
Fort, B., & Mellier, Y. 1994, A&A Rev., 5, 239  
Fukugita, M., Shimasaku, K., & Ichikawa, T. 1995, PASP, 107, 945  
Hall, P. B., et al. 2000, AJ, 120, 1660  
Hammer, F., et al. 1997, ApJ, 481, 49  
Kennicutt, R. C., Jr. 1983, ApJ, 272, 54  
—. 1992a, ApJS, 79, 255  
—. 1992b, ApJ, 388, 310  
—. 1998, ARA&A, 36, 189  
Kron, R. G. 1980, ApJS, 43, 305  
Lémonon, L., Pierre, M., Cesarsky, C. J., Elbaz, D., Pelló, R., Soucail, G., & Vigroux, L. 1998, A&A, 334, L21  
Mellier, Y., Fort, B., & Kneib, J.-P. 1993, ApJ, 407, 33  
Montgomery, K. A., Marschall, L. A., & Janes, K. A. 1993, AJ, 106, 181  
Osterbrock, D. E., & Martel, A. 1992, PASP, 104, 76

- Paczynski, B. 1987, *Nature*, 325, 572  
Poggianti, B. M. 1997, *A&AS*, 122, 399  
Pointecouteau, E., Giard, M., Benoit, A., Désert, F. X., Aghanim, N., Coron, N., Lamarre, J. M., & Delabrouille, J. 1999, *ApJ*, 519, L115  
Sahu, K. C., et al. 1998, *ApJ*, 492, L125  
Salpeter, E. E. 1955, *ApJ*, 121, 161  
Schindler, S., et al. 1995, *A&A*, 299, L9  
Schindler, S., Hattori, M., Neumann, D. M., & Böhringer, H. 1997, *A&A*, 317, 646  
Schlegel, D. J., Finkbeiner, D. P., & Davis, M. 1998, *ApJ*, 500, 525  
Smail, I., Ellis, R. S., Aragón-Salamanca, A., Soucail, G., Mellier, Y., & Giraud, E. 1993, *MNRAS*, 263, 628  
Stone, R. P. S., & Baldwin, J. A. 1983, *MNRAS*, 204, 347  
Tonry, J., & Davis, M. 1979, *AJ*, 84, 1511  
White, D. A., & Fabian, A. C. 1995, *MNRAS*, 273, 72  
Yee, H. K. C., Ellingson, E., & Carlberg, R. G. 1996, *ApJS*, 102, 269